A Lead PhosphoMolybdenum Purple Bronze: $Pb_{0.9}PMo_5O_{17}$

A. Leclaire,* J. Chardon, S. Boudin, J. Provost, and B. Raveau

Laboratoire CRISMAT, UMR CNRS ISMRA 6508, 6 bd Maréchal Juin, 14050 Caen Cedex, France

Received February 19, 2002. Revised Manuscript Received May 27, 2002

A phosphomolybdenum bronze containing lead, $Pb_{0.9}PMo_5O_{17}$, has been synthesized for the first time. It crystallizes in the space group $P\bar{3}m1$, with $a = 5.415(1)$ Å and $c = 13.476(2)$ Å. Its crystal structure, close to that of the charge density wave (CDW) bronze $Na_{0.9}$ Mo_6 O_{17}, differs from the latter by the occupation of one crystallographic site by P and Mo simultaneously and by the position of Pb^{2+} cations, which are distributed over 12 split sites because of the stereoactivity of the $6s^2$ lone pair of Pb^{2+}. The calculation of the density of states predicts a metallic behavior in agreement with the Pauli paramagnetic susceptibility for $T > 75$ K. The resistivity measured versus T on a polycrystalline bar is explained as the result of grain boundary effect, preventing the metal-like behavior from being evidenced. No sign of a CDW could be detected.

Introduction

Among the numerous bronzes, the purple molybdenum bronzes $A_{0.9}Mo_6O_{17}$ with A = Na, K, Rb, Tl (see for a review refs 1 and 2) and the phosphate tungsten bronze $(PO_2)_4(WO_3)_{2m}$ and $A_x(PO_2)_4(WO_3)_{2m}$ (see for a review refs 3−5) have been intensively investigated in recent years for their charge density wave (CDW) properties (see for a review refs 6 and 7). The latter properties originate from the bidimensional character of the structure induced by the presence in the same framework of MoO_6 or WO_6 octahedra and MoO_4 or PO_4 tetrahedra. The association of PO_4 tetrahedra and MoO_6 octahedra should allow similar frameworks to be generated. Surprisingly, only one phosphomolybdenum bronze having a univalent cation (A = Ag), $Ag_{0.8}$ $(PO_2)_4(MoO_3)_{12}$, could be synthesized.[8] Moreover, no bronze belonging to these structural families and containing bivalent cations is known to date. For this reason we have revisited the Pb−Mo−P−O phase diagram.

In the present paper, we show the possible stabilization of lead molybdenum purple bronze by associating phosphorus with molybdenum in the tetrahedra. The structure of this new bronze, $Pb_{0.9}PMo_5O_{17}$, is described and compared to those of $Na_{0.9}$ Mo_6 O_{17}[9] and $K_{0.9}$ Mo_6 O_{17}.[10] The transport and magnetic properties are investigated and discussed.

Experimental Section

Synthesis and Crystal Growth. Single crystals of the title compound were grown from a mixture of nominal composition $PbPMo_6O_{20}$. First $PbCO_3$, $H(NH_4)_2PO_4$, and MoO_3 were mixed in an agate mortar in the molar ratio 2:2:5.666 and heated at 600 K in a platinum crucible to decompose the ammonium phosphate and the carbonate. In a second step the resulting mixture was crushed, added to metallic molybdenum powder, that is, to 0.333Mo with 2% weight of KCl as the flux agent, sealed in an evacuated silica ampule, then heated for 12 h at 813 K, cooled at 3.5 K/h to 473 K, and finally quenched to room temperature. Purple crystals were extracted from a dark product.

To obtain a pure phase in the form of bulk polycrystalline powders, a similar process was used. First, a mixture of $PbCO_3$, $H(NH_4)_2PO_4$, and MoO_3 with the molar ratios 0.92:1:4.833 was heated in air at 600 K. The resulting mixture was added to metallic molybdenum powder (0.1666Mo), sealed in an evacuated silica ampule, heated for 12 h at 923 K, and finally cooled in the same way as for the crystal growth.

The X-ray powder diffraction pattern of this sample showed that it is practically a single phase. The pattern could indeed be indexed with the cell parameters obtained from the single-crystal X-ray structure determination.

The energy-dispersive spectroscopy (EDS) carried out with an analyzer Link Isis (Oxford) mounted on a Philips XL30 FEG allowed the cationic composition "$Pb_{0.9}PMo_5$" to be confirmed.

Crystal Structure Determination. A purple plate crystal with dimensions $0.086 \times 0.086 \times 0.014$ mm^3 was selected for

* To whom correspondence should be addressed.

(1) Wadsley, A. D. In *Non-Stoichiometric Compounds*; Mandelcorn, L., Ed.; Academic Press: New York, 1964; Chapter 3.
(2) Hagenmuller, P. In *Progress in Solid State Chemisty*; Reiss, H., Eds.; Pergamon Press: New York, 1971; Vol. 5, Chapter 3.
(3) Raveau, B. *Proc. Indian Nat. Sci. Acad.* **1986**, *52A*, 67−101; *Proc. Indian Nat. Sci.* **1986**, *96*, 419−448.
(4) Borel, M. M.; Goreaud, M.; Grandin, A.; Labbé, Ph.; Leclaire, A.; Raveau, B. J. *Solid State Inorg. Chem.* **1991**, *28*, 93−129.
(5) Rao, C. N. R.; Raveau, B. *Transition Metal Oxides*, 2nd ed.; Wiley-VCH: New York, 1998.
(6) Greenblatt, M. In *Physics and Chemistry of Low-Dimensional Inorganic Conductors*; Schlenker, C., Dumas, J., Greenblatt, M., Van Smaalen, S., Eds.; NATO ASI Series. Series B, Physics; Plenum Press: New York, 1996; Vol 354, Chapter 2. Schlenker, C. In *Physics and Chemistry of Low-Dimensional Inorganic Conductors*; Schlenker, C., Dumas, J., Greenblatt, M., Van Smaalen, S., Eds.; NATO ASI Series. Series B, Physics; Plenum Press: New York, 1996; Vol 354, Chapter 8.
(7) *Low-Dimensionnal Electronic Properties of Molybdenum Bronzes and Oxides*; Schlenker, C., Ed.; Kluwer Academic Publishers: Dordrecht, 1989.
(8) Ledain, S.; Leclaire, A.; Borel, M. M.; Provost, J.; Raveau, B. *J. Solid State Chem.* **1998**, *140*, 128−133.
(9) Onoda, M.; Matsuda, Y.; Sato, M. *J. Solid State Chem.* **1987**, *69*, 65−75.
(10) Vincent, H.; Ghedira, M.; Marcus, J.; Mercier, J.; Schlenker, C. *J. Solid State Chem.* **1983**, *47*, 113−121.

10.1021/cm020217n CCC: $22.00
Published on Web 06/28/2002

Table 1. Summary of Crystal Data, Intensity Measurement, and Structure Refinement for $Pb_{0.92}P_{1.07}Mo_{4.93}O_{17}$

chemical formula	$Pb_{0.9164}P_{1.069}Mo_{4.931}O_{17}$
molecular weight	968.059D
crystal system	trigonal
space group	$P\bar{3}m1$ (164)
cell dimensions	$a = 5.415(1)$ Å
	$b = 5.415(1)$ Å
	$c = 13.476(2)$ Å
cell volume	342.2(1) Å^3
Z	1
density	4.697 g·cm^{-3}
μ	16.907 mm^{-1}
T_{min}	0.3429
$T_{max.}$	0.7949
measured reflections	5769
reflections with $I > 3\sigma(I)$	1144
independent data with $I > 3\sigma(I)$	329
R_{inter}	0.0333
temperature of the data collections	21 °C
number of variable	40
$R(F_o)$	0.0390
R_W	0.0245

the structure determination after tests made with film techniques on a Weissenberg camera. The cell parameters (Table 1) were determined with a least-squares method using 25 reflections with $18° < \theta < 22°$. The data were recorded at room temperature on an Enraf-Nonius CAD 4 diffractometer using Mo Kα radiation ($\lambda = 0.71073$ Å) isolated with a graphite monochromator. Intensities were checked by monitoring three standard reflections every hour. No significant deviations in intensities were observed. The intensity data were corrected for the Lorentz, polarization, and absorption effects. The absorption corrections were computed by the Gaussian method, taking into consideration the shape of the crystal. The reflections are consistent with the $P\bar{3}m1$ or $P3m1$ space groups. The refinements were successful with the centrosymmetric space group $P\bar{3}m1$.

The structure was solved with the heavy atom method. The full-matrix least-squares refinements were performed on F weighted by $1/\sigma(F)^2$ with the JANA98 package.[11] The latter leads to $R = 0.0390$ and $R_w = 0.0245$ and to the atomic parameters of Table 2.

Magnetic and Transport Measurements

The measurements were carried out on a parallelepipedic bar 12 × 1.5 × 1.5 mm^3 of $Pb_{0.9}PMo_5O_{17}$, sintered at 873 K under vacuum. The same sample was used for both transport and magnetic measurements.

The magnetic susceptibily was first measured between 5 and 300 K under a magnetic field $B = 0.3$ T with a Quantum Design MPMS (Magnetic Properties Measurement System).

Four pure indium dots were then deposited on the bar using an ultrasonic-assisted soldering setup. Four 25-μm-diameter gold wires were indium-soldered on the dots. The electrical resistivity was measured by the standard four-probes measurement method between 5 and 325 K with a Quantum Design PPMS (Physical Properties Measurement System).

Results and Discussion

Description of the Structure. The host lattice [Mo_5PO_{17}] of this lead phosphomolybdenum bronze is very similar to those of the purple bronzes $Na_{0.9}Mo_6O_{17}$[9] and $K_{0.9}Mo_6O_{17}$,[10] as shown from the projection of the structure along $\vec{a}$ (Figure 1). It consists of ReO_3-type slabs of corner-sharing MoO_6 octahedra, which are four octahedra thick. These layers oriented parallel to the

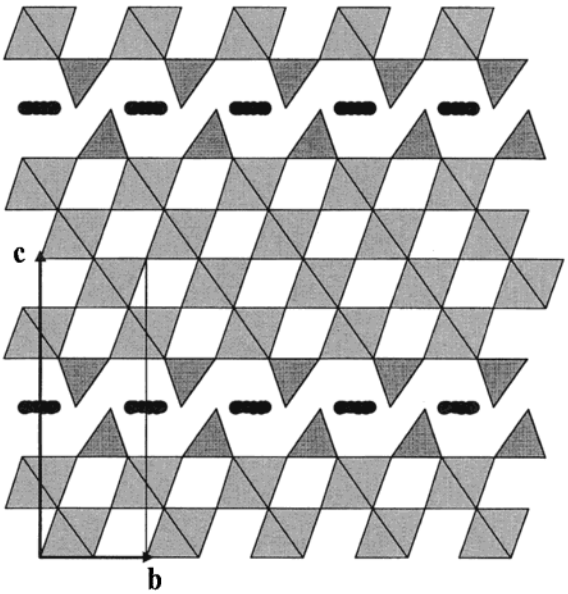

Figure 1. Projection of the structure of the lead phosphomolybdenum purple bronze $Pb_{0.9}PMo_5O_{17}$ along $\vec{a}$.

(001) plane are bordered with PO_4 and MoO_4 tetrahedra, forming mixed $[Mo_5PO_{17}]_\infty$ layers. The latter shows a great similarity with those observed in the monophosphate tungsten bronzes $A_x(PO_2)_4(WO_3)_{2m}$.[3−5] The $(Mo_5PO_{17})_\infty$ layers can indeed be described by the assemblage of (012) ReO_3-type ribbons, which are four octahedra wide (Figure 2a), similar to the (102) ribbons forming the ReO_3-type layers of $K_{0.8}P_4W_8O_{32}$ (Figure 2b), $m =$ 4-member of the $K_x(PO_2)_4(WO_3)_{2m}$ series.[12] In contrast to the phosphate tungsten bronzes, two successive $[Mo_5PO_{17}]_\infty$ layers are disconnected so that the $MoO_4(PO_4)$ tetrahedra exhibit one free apex. The lead cations sit between two successive layers at the level of the $MoO_4(PO_4)$ tetrahedra, suggesting a more prononced bidimensionnal character for the purple bronzes than for the monophosphate tungsten bronzes.

The originality with respect to $K_{0.9}Mo_6O_{17}$ and to $Na_{0.9}Mo_6O_{17}$ stems from the following two features: first, the tetrahedral sites are half occupied by molybdenum and half by phosphorus and, second, the lead cations are distributed differently than the Na^+ and K^+ cations. The random distribution of P and Mo in the same crystallographic site seems to be a unique feature in molybdenum phosphates: it has not been encountered to date, to our knowledge, in contrast to vanadium phosphates for which several examples are known.[13,14] The "delocalization" of Pb^{2+} over 12 split sites, at 7.64% occupied (Figure 3), in contrast to a unique site occupied at 90% for Na^+ and K^+, is certainly related to the stereoactivity of the $6s^2$ lone pair of Pb^{2+}.

The distortion of the MoO_6 octahedra is similar to that observed in the sodium and potassium purple bronzes, that is, characterized by three short Mo−O bonds as opposed to three longs ones (Table 3). Nevertheless, it must be pointed out that the Mo(1) octahedra linked to MoO_4 (PO_4) tetrahedra are more distorted in our Pb−

(11) Petricek, V.; Dusek, M. *JANA 98*; Institute of Physics, Academy of Sciences of the Czech Republic, 1998.

(12) Girault, J. P.; Goreaud, M.; Labbé, Ph.; Raveau, B. *J. Solid State Chem.* **1982**, *44*, 407−414.

(13) Idler, K. L.; Calvo, C. *Can. J. Chem.* **1975**, *53*, 3665.

(14) Boudin, S.; Chardon, J.; Daturi, M.; Raveau, B. *J. Solid State Chem.* **2001**, *159*, 239.

Table 2. Atomic Coordinates of $Pb_{0.92}P_{1.07}Mo_{4.93}O_{17}$

	X	*Y*	*Z*	U_{eq}	occup.
Mo(1)	0.000000	0.000000	0.22879(9)	0.0103(6)	1
Mo(2)	0.333333	0.666667	0.9256(1)	0.0106(4)	1
Mo+P	0.333333	0.666667	0.3787(1)	0.0110(9)	0.466(1)Mo + 0.534(1)P
Pb(1)	0.1063(7)	0.140(3)	0.500(2)	0.019(3)	0.0764(3)
O(1)	0.500000	1.000000	1.000000	0.013(4)	1
O(2)	−0.1661(5)	−*X*	0.1643(4)	0.019(3)	1
O(3)	2*Y*	0.8276(7)	0.3352(4)	0.024(3)	1
O(4)	0.333333	0.666667	0.4970(7)	0.031(4)	1

$U_{eq} = (\Sigma U_{ii})/3$

	U_{11}	U_{22}	U_{33}	U_{12}	U_{13}	U_{23}
Mo(1)	0.0113(6)	0.0113(6)	0.0084(7)	0.0056(3)	0.000000	0.000000
Mo(2)	0.0104(4)	0.0104(4)	0.0109(5)	0.0052(2)	0.000000	0.000000
Mo+P	0.0097(8)	0.0097(8)	0.013(1)	0.0048(4)	0.000000	0.000000
Pb(1)	0.019(7)	0.023(2)	0.0158(8)	0.016(2)	−0.003(4)	0.002(2)
O(1)	0.011(4)	0.019(5)	0.009(3)	0.009(3)	0.001(2)	0.003(4)
O(2)	0.021(3)	0.021(3)	0.015(3)	0.015(4)	−0.006(1)	0.006(1)
O(3)	0.027(3)	0.031(2)	0.014(3)	0.014(1)	0.009(2)	0.004(1)
O(4)	0.032(4)	0.032(4)	0.029(6)	0.016(2)	0.000000	0.000000

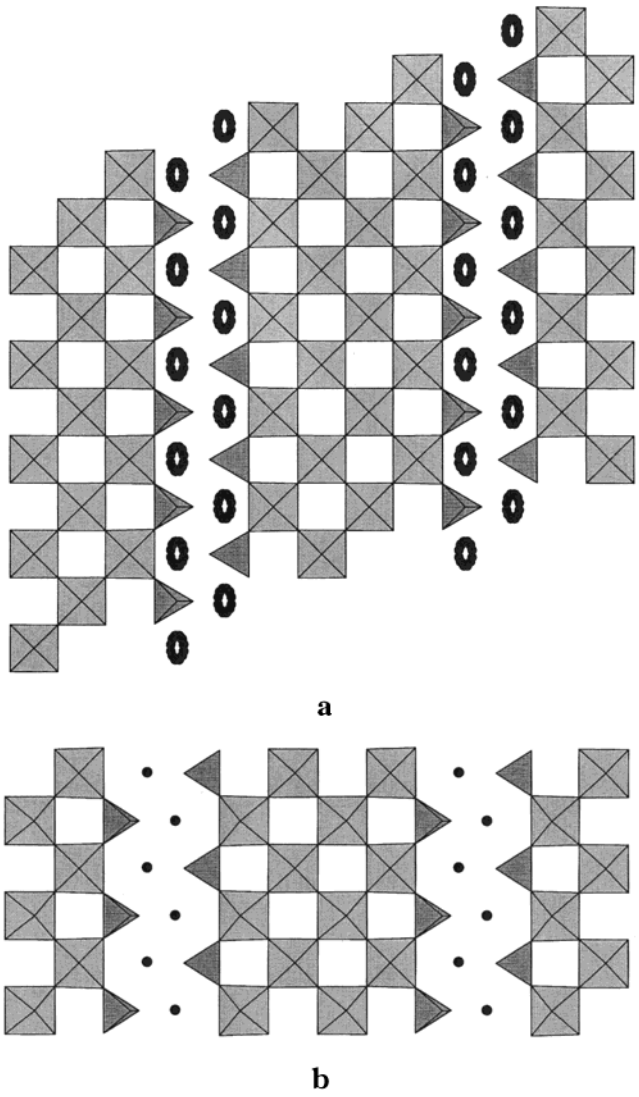

Figure 2. The four octahedra wide and one octahedron thick ribbons parallel to (012) in the $Pb_{0.9}PMo_5O_{17}$ structure (a) and to (102) in the $K_{0.8}P_4Mo_8O_{32}$ structure (b).

purple bronze (Mo−O bonds ranging from 1.784 to 2.162 Å) than in the Na−bronze (from 1.771 to 2.122 Å) and in the K−bronze (from 1.771 to 2.101 Å), whereas the Mo(2) octahedra, which sit inside the octahedral layers, are less distorted in the Pb−bronze (Mo−O bonds ranging from 1.857 to 1.982 Å) than in the Na−bronze (from 1.865 to 2.027 Å) and in the K−bronze (from 1.869 to 2.028 Å).

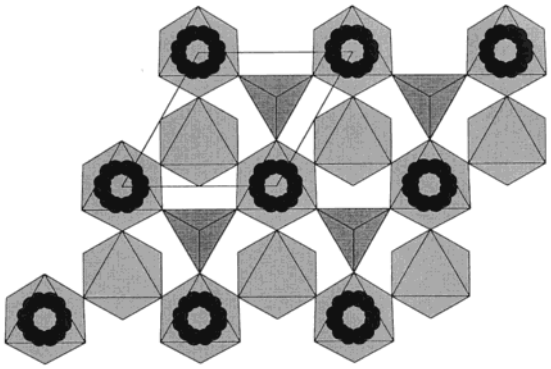

Figure 3. Projection of a double layer of MoO_6 octahedra and MoO_4 and PO_4 tetrahedra along $\vec{c}$, and the corresponding 12-fold sites of lead forming a crown (small black circles)

Table 3. Interatomic Distances (Å) and Angles (deg) in $Pb_{0.92}P_{1.07}Mo_{4.93}O_{17}$[a]

Mo(1)	**O(2)**	**O(2^{i})**	**O(2^{ii})**	**O(3^{iii})**	**O(3^{iv})**	**O(3^{v})**
O(2)	**1.784(4)**	2.699(5)	2.699(5)	2.798(7)	3.923(8)	2.797(7)
O(2^{i})	98.3(2)	**1.784(4)**	2.699(5)	2.798(7)	2.798(7)	3.923(8)
O(2^{ii})	98.3(2)	98.3(2)	**1.784(4)**	3.923(8)	2.798(7)	2.798(7)
O(3^{iiii})	89.8(2)	89.8(2)	167.6(8)	**2.162(5)**	2.802(8)	2.802(8)
O(3^{iv})	167.6(2)	89.8(2)	89.8(2)	80.8(2)	**2.162(5)**	2.802(8)
O(3^{v})	89.8(2)	167.6(2)	89.8(2)	80.8(2)	80.8(2)	**2.162(5)**

Mo(2)	**O(1)**	**O(1^{vi})**	**O(1^{vii})**	**O(2^{viii})**	**O(2^{ix})**	**O(2^{x})**
O(1)	**1.857(1)**	2.708(1)	2.708(1)	2.712(5)	3.836(5)	2.712(5)
O(1^{vi})	93.6(1)	**1.857(1)**	2.708(1)	2.712(5)	2.712(5)	3.836(5)
O(1^{vii})	93.6(1)	93.6(1)	**1.857(1)**	3.836(5)	2.712(5)	2.712(5)
O(2viii)	89.8(1)	89.8(1)	175.0(2)	**1.982(4)**	2.717(5)	2.717(5)
O(2^{ix})	175.0(2)	89.8(1)	89.8(1)	86.5(2)	**1.982(4)**	2.717(5)
O(2^{x})	89.8(1)	175.0(2)	89.8(1)	86.5(2)	86.5(2)	**1.982(4)**

MoP(1)	**O(3)**	**O(3^{vi})**	**O(3^{v})**	**O(4)**
O(3)	**1.619(5)**	2.614(5)	2.614(5)	2.651(9)
O(3^{vi})	107.7(2)	**1.619(5)**	2.614(5)	2.651(9)
O(3^{v})	107.7(2)	107.7(2)	**1.619(5)**	2.651(9)
O(4)	111.2(2)	111.2(2)	111.2(2)	**1.594(9)**

[a] The M−O distances are on the diagonal and the O...O distances above it and the O−M−O angle under it.

The interatomic distances observed in the tetrahedra (Table 3) are significantly smaller than those of the sodium and potassium purples bronzes. They correspond to intermediate values between the Mo−O bonds and

Table 4. Lead Coordination in $Pb_{0.92}P_{1.07}Mo_{4.93}O_{17}$

Pb(1)−O(3^{v})	2.43(2) Å	Pb(1)−O(3^{iv})	2.92(2) Å
Pb(1)−O(4)	2.48(2) Å	Pb(1)−O(4^{viii})	3.04(2) Å
Pb(1)−O(3^{xi})	2.53(2) Å	Pb(1)−O(3^{iii})	3.10(2) Å
Pb(1)−O(4^{xi})	2.67(2) Å	Pb(1)−O(3^{xiii})	3.19(2) Å
Pb(1)−O(3^{xii})	2.74(2) Å		

Symmetry Codes

i: $-y, x-y, z$	viii: $-x, 1-y, 1-z$
ii: $-x+y, -x, z$	ix: $y, -x+y, 1-z$
iii: $x-1, y-1, z$	x: $1+x-y, 1+x, 1-z$
iv: $1-y, x-y, z$	xi: $1-x, 1-y, 1-z$
v: $1-y, 1-x, z$	xii: $y-1, -x+y, 1-z$
vi: $1-y, 1+x-y, z$	xiii: $y-1, x-1, 1-z$
vii: $-x+y, 1-x, z$	

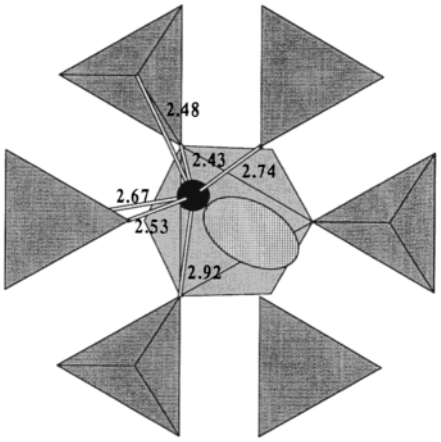

Figure 4. Representation of one lead position and its six nearest neighbors, with the possible orientation of the $6s^2$ lone pair.

P−O bonds in the tetrahedra, in perfect agreement with the simultaneous occupation of those tetrahedral sites by P and Mo.

The bond valence sums calculated with the universal constant determined by Zocchi[15] for molybdenum lead to formal charges of 5.28 and 5.36 for Mo(1) and Mo(2), respectively, in agreement with the average value 5.30 deduced from the chemical formula. Note that this average valence of molybdenum in the octahedral layers is close to that obtained for $Na_{0.9}Mo_6O_{17}$ and $K_{0.9}Mo_6O_{17}$] (5.275), supposing Mo^{6+} in the tetrahedra.

The Pb−O distances (Table 4) show that each Pb^{2+} cation has five Pb−O distances smaller than 2.9 Å so that its coordination can be considered as 5-fold or 6-fold. But more importantly, it can be seen from one of the 12 equivalent positions possible for Pb^{2+} (Figure 4) that its five (or even six) nearest oxygen neighbors are sitting on a same side, leaving more space for its $6s^2$ lone pair, which should be oriented in the opposite direction. This explains the splitting of the Pb sites out of the barycenter of the surrounding polyhedra, forming a crown (Figure 2) to satisfy the lone pair extension.

Magnetic and Transport Properties

Bearing in mind the great structural similarity of the $Pb_{0.9}PMo_5O_{17}$ with the purple bronzes $Na_{0.9}Mo_6O_{17}$ and $K_{0.9}Mo_6O_{17}$, and the very similar average molybdenum valency in the three compounds (5.275 to be compared to 5.30), metallic properties and even charge density

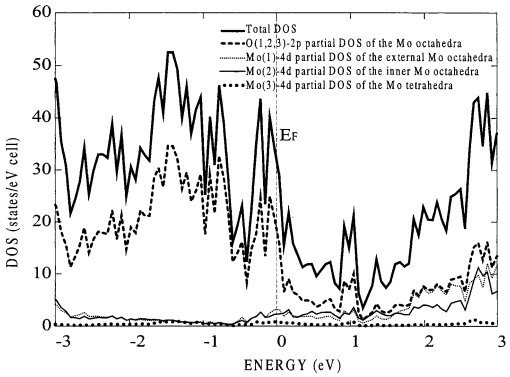

Figure 5. Total, Mo(3) 4d, Mo(1) 4d, Mo(2) 4d, and O(1,2,3) 2p partial DOS of $PbPMo_5O_{17}$.

wave properties should be expected for this new lead phosphomolybdenum purple bronze.

To support the above hypothesis, electronic structure calculations were carried out using the TB-LMTO-ASA method (tight binding linearized muffin tin orbital within the atomic sphere approximation) with Andersen's Program.[16] k space integrations employed the tetrahedron method using more than 140 k points within the irreducible point of the Brillouin zone. For the sake of modelization, the splitting of the Pb^{2+} cations on the different sites is not considered, that is, Pb^{2+} was located on the 1(b) site, and an ordered arrangement of the MoO_4 and PO_4 tetrahedra was considered in each (001) layer (one PO_4 tetrahedron being surrounded by four MoO_4 tetrahedra and vice versa). The so obtained density of state (DOS) of $PbPMo_5O_{17}$ (Figure 5) clearly indicates that this phase is metallic with DOS at the Fermi level. The partial DOS plotted for the Mo(3) 4d orbitals of the MoO_4 tetrahedra and for the Mo(1) 4d, Mo(2) 4d, and O(1,2,3) 2p orbitals of the MoO_6 octahedra show at E_F the absence of DOS for the tetrahedral sites against important contributions of the Mo and O atoms of each MoO_6 octahedron, revealing that electronic conduction occurs through the whole octahedral layer. This result is in agreement with the bond valence calculations, which indicate that the single 4d electrons of the Mo atoms are delocalized over all the octahedral sites, leading to very close valencies (5.28 for Mo(1) and 5.31 for Mo(2)). This behavior differs slightly from that of the CDW $K_{0.9}Mo_6O_{17}$ bronze whose itinerant electrons are mainly delocalized over the central Mo(2) octahedra.[17,18]

The evolution of the molar magnetic susceptibility χ_M versus temperature (Figure 6) shows that at high temperature χ_M is very small and temperature-independent. Such a behavior is characteristic of Pauli paramagnetism and supports strongly the metallic properties expected for this phase. Nevertheless, one observes an upturn at lower temperature ($T < 75$ K), which can be ascribed to the presence of a paramagnetic impurity (containing for example Mo^{5+}) at very low concentration. The value of the molar susceptibility at 5 K, $\chi_M(5\text{ K}) = 0.002$ emu/mol, corresponds indeed

(15) Zocchi, F. *Solid State Sci.* **2001**, *3*, 383.

(16) Andersen, O. K.; Jespen, O. *TB-LMTO-ASA, Version 47*; Stuggart: Germany, 1996.

(17) Whangbo, M. H.; Canadell, E.; Schlenker, C. *J. Am. Chem Soc.* **1987**, *109*, 6308−6313.

(18) Whangbo, M. H.; Canadell, E.; Foury, P.; Pouget, J. P. *Science* **1991**, *25*, 96−98.

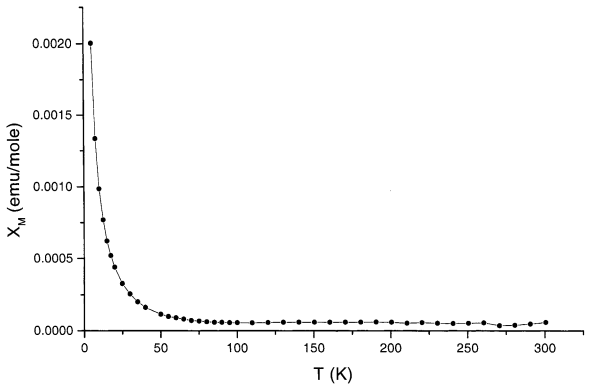

Figure 6. Magnetic susceptibility curve $\chi(T)$ of $Pb_{0.9}PMo_5O_{17}$.

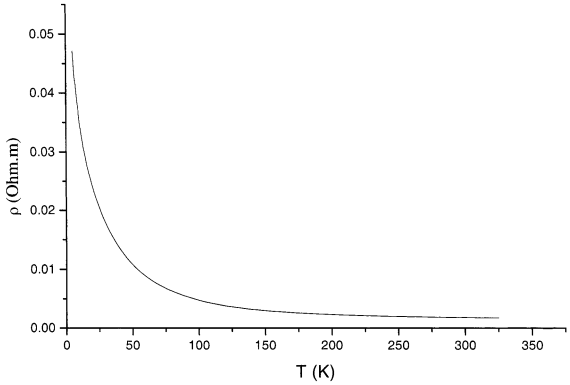

Figure 7. Resistivity curve $\rho(T)$ of $Pb_{0.9}PMo_5O_{17}$.

approximately to the presence of 2.5% Mo^{5+} ion per molybdenum mole. This explains that the corresponding impurity phase cannot be detected for XRPD patterns.

The evolution of the resistivity versus temperature (Figure 7) does not exhibit the expected metallic behavior. This $\rho(T)$ curve is rather similar to that observed for the blue bronze $Tl_{0.30}MoO_3$,[19] which exhibits a metal−insulator transition at $T = 180$ K. However, the $\rho(T)$ curve of $Pb_{0.9}PMo_5O_{17}$ does not show a metallic conductivity at high temperature, contrary to $Tl_{0.30}MoO_3$, and moreover we do not detect any anomaly of the magnetic susceptibility on the $\chi(T)$ curve (Figure 6), in contrast to $Tl_{0.3}MoO_3$ where magnetic susceptibility shows a decrease at the metal−insulator transition. At this point, the possibility of semiconducting behavior can be considered. Nevertheless, a logarithmic plot of the resistivity versus reciprocal temperature leads to a strong curvature for Log $\rho(1/T)$ in the whole temperature range, demonstrating that this phase is not a standard semiconductor.

The rather low but not metallic resistivity, ranging from $\rho = 0.047$ Ω-m at $T = 5$ K to $\rho \simeq 1.8 \times 10^{-3}$ Ω-m at $T = 300$ K, can be explained in two different ways.

We can first suppose that the grains of the bars are in fact metallic, as suggested by the electronic structure calculation and by the average molybdenum valency compared to that of molybdenum in metallic bronzes. In this hypothesis, the activated character of the conductivity should be related to a grains boundary effect. A semiconducting phase should be present as an impurity at the grain boundary, which hinders the metallic conductivity to be evidenced. This first interpretation is in agreement with the susceptibility measurements, the metallic grains of the sample being responsible for the Pauli paramagnetism observed above 75 K, whereas the impurity phase located at the grains boundary is at the origin of susceptibility obtained at low temperature.

The second explanation that can be equally invoked concerns the disorder present in this compound. There is disorder in the tetrahedral Mo and P sites and in the Pb sites. As indicated above, the splitting of Pb on the different sites was not considered (Pb^{2+} was located on the 1(b) site for calculations) and an ordered distribution of Mo and P tetrahedral sites was also considered. The random potential due to the disorder can in fact induce an activated conductivity contrary to the metallic character deduced from the ordered system. Moreover, the disorder in the system should be detrimental to the transition to a charge density wave despite the similarities of the system with $Na_{0.9}Mo_6O_{17}$ and $K_{0.9}Mo_6O_{17}$,

In conclusion, a purple bronze containing lead and phosphorus, $Pb_{0.9}Mo_5PO_{17}$, has been synthesized for the first time. The DOS calculations and magnetic susceptibility could suggest that this phase is a metallic conductor but the measured conductivity is high but activated. Moreover, no sign of transition to a charge density wave state has been detected in the magnetic and transport measurement. Single-crystal growth will be carried out to choose between the two interpretations invoked to explain the activated character of the conductivity and understand the relationships between the physical properties and the structure of this bronze. The route is also open to the discovery of others members of the series, using phosphorus as a stabilizer.

CM020217N

(19) Ramanujachary, K. V.; Collins, B. T.; Greenblatt, M.; Waszczak, J. V. *Solid State Commun.* **1986**, *59*, 647.